RSC Advances

ROYAL SOCIETY OF CHEMISTRY

www.rsc.org/advances

Synergistic Effects of Magainin 2 and PGLa on Their Heterodimer Formation, Aggregation, and Insertion into the Bilayer

Eol Han, Hwankyu Lee*

Department of Chemical Engineering, Dankook University,

Yongin, 448-701, South Korea

*Corresponding author

Email: leeh@dankook.ac.kr

Abstract

We performed coarse-grained molecular dynamics simulations of antimicrobial peptides PGLa and magainin 2 in lipid bilayers. PGLa peptides or mixtures of PGLa and magainin 2 were initially widely spaced or clustered above the bilayer surface with different heterodimeric orientations (parallel or antiparallel). Simulations show that the presence of magainin 2 promotes more tilting and insertion of PGLa into the bilayer, indicating the synergistic effect. Magainin 2 interact with lipid headgroups and thus stay horizontally on the bilayer surface, while PGLa insert into the bilayer, leading to more tilted conformation, in agreement with recent NMR experiments. In particular, for the systems with the initially antiparallel-oriented heterodimers or with the neutrally mutated magainin 2, much fewer parallel heterodimers form, and PGLa peptides are less tilted and inserted, indicating that the formation of parallel heterodimers is important for the PGLa insertion, as suggested in experiments. Peptides aggregate in the mixture of PGLa and magainin 2, but not in the system without magainin 2, indicating that magainin 2 induce the peptide aggregation, which is required for the pore formation. These simulation findings agree with the experimental observations of the heterodimer formation as well as different positions of PGLa and magainin 2 in the bilayer, which seem to conflict. These conflicting results can be explained by the synergistic mechanism that magainin 2 form parallel heterodimers with PGLa and induce the aggregation of heterodimers, leading to the formation of pores, where magainin 2 tend to interact with the bilayer surface, while PGLa are tilted and inserted into the hydrophobic region of the bilayer.

Introduction

Antimicrobial peptides (AMPs), which consist of <50 amino acid residues, are found in eukaryotic organisms for the immune defense against bacterial pathogens.[1, 2] Since AMPs are cationic and amphipathic, they tend to interact with anionic bacterial membranes rather than with neutral animal membranes, showing great potential for use as novel antibiotics.[3-5] To improve their efficiency in this biomedical application, the interactions between AMPs and cell membranes have been widely studied.[6-17] In particular, experiments have shown the synergistic effects of mixtures of different AMPs on antimicrobial activity.[18-22]

Williams et al. found that a mixture of magainin 2 and PGLa induces much stronger antimicrobial activity than does either magainin 2 or PGLa, indicating their synergistic effect.[23] Also, Vaz Gomes et al. and Westerhoff et al. found that magainin 2 and PGLa form the complex, yielding the greatest synergistic effect at a molar ratio of 1:1.[24, 25] To understand the mechanism for this synergistic effect, the Matsuzaki group characterized the conformation of PGLa-magainin complexes and their interactions with lipid bilayers, which showed that parallel-oriented heterodimers significantly increase the pore formation and stability, suggesting that heterodimers of PGLa and magainin 2 induce pore formation in lipid bilayers.[26-28] To investigate the position and orientation of the PGLa-magainin 2 heterodimers in the bilayer, Ulrich and coworkers performed solid-state NMR experiments and showed that the presence of magainin 2 increases tilt angles of PGLa, indicating the deeper insertion of the C-terminal group of PGLa.[29, 30] In particular, they observed that magainin 2 peptides mostly stay on the bilayer surface, while PGLa peptides insert into the hydrophobic region of the bilayer,[31] implying that the inserted peptides may not retain the side-by-side heterodimeric structure, which was also supported by Salnikov and Bechinger's experiments.[32] They also showed that these synergistic effects on the

PGLa insertion depend on membrane curvature (positive vs. negative) rather than membrane thickness, which conflicts with Salnikov and Bechinger's experiments that suggested that magainin 2 may reduce membrane thickness and thus promote the deeper PGLa insertion and pore formation. These experiments clearly showed that magainin 2 and PGLa form the parallel heterodimer and promote the deeper insertion of PGLa into the bilayer, but also showed different positions of PGLa and magainin 2, suggesting that magainin 2 and PGLa may not retain the side-by-side heterodimeric structure. Thus, these conflicting experimental observations and the mechanism for the synergistic effect are still not well understood. To resolve this, the interaction between those AMPs and lipid bilayers needs to be studied at nearly the atomic scale.

Molecular dynamics (MD) simulations have been able to explore the interactions of magainin 2 and PGLa with lipid bilayers. Simulations have shown that magainin peptides bind to the bilayer surface and insert into the lipid-tail region, which disorder lipids and thus induce pore formation, depending on the structure, sequence, and concentration of peptides,[33-41] ion concentration,[42] and polymer conjugation.[43] In particular, coarse-grained (CG) MD simulations captured the experimentally proposed toroidal pores.[36-39] For PGLa, Ulrich and coworker's simulations recently showed the formation of PGLa monomers and dimers, respectively, at low and high concentrations.[44] They also found that dimers have the higher tilt angles than do monomers, indicating the effect of the dimeric structure on the insertion into the bilayer. These MD simulations have revealed atomic-scale insights into the structure and dynamics of either PGLa or magainin 2 and its interaction with the lipid bilayer, but the mixtures of PGLa and magainin 2 have not yet been simulated to understand their synergistic effect on the insertion and pore formation.

In this study, we therefore perform MD simulations of the mixture of magainin 2 and

PGLa in lipid bilayers to understand their synergistic effects on the insertion into the bilayer. The PGLa-magainin 2 dimers were initially aligned in parallel or antiparallel, and the systems with mutated magainin 2 or without magainin 2 are also simulated. The orientation and position of peptides in lipid bilayers are analyzed by calculating the tilt angles and the distances from the bilayer center, which compare favorably with experiments. In particular, we find the dependence of the tilted conformation, aggregation, and insertion of PGLa on the presence of magainin 2 and the heterodimer orientation (parallel or antiparallel), which is rationalized by analyzing the interactions of PGLa, magainin 2, and lipids. We will show that these results help explain the conflicting experimental results regarding the dimer formation and different positions of PGLa and magainin 2.

Methods

All simulations and analyses were performed using the GROMACS4.5.5 simulation package.[45-48] Magainin 2 (GIGKF LHSAK KFGKA FVGEI MNS), PGLa (GMASK AGAIA GKIAK VALKA L) and dilauroylglycerophosphocholine (DLPC) lipids were modeled directly from the "MARTINI" CG force field (FF),[49-51] which lumps a few (three or four) heavy atoms into each CG bead. The C-terminal group of PGLa was protonated (neutralized), while both N- and C-terminal groups of magainin 2 were unmodified, leading to net charges of +5 and +3, respectively, for PGLa and magainin 2 (Figure 1), which match the charge states of the experimental peptides.[31] The mutated magainin 2 was generated by replacing the charged beads of two anionic residues with neutral nonpolar beads. Note that in this CG model the helical structure of peptides is fixed and thus does not change for whole simulation time. However, this should not significantly influence simulation results, since experiments also showed that peptides

retain their helical structure in membranes.[52, 53] To test the lipid FF, the bilayer composed of 512 DLPC lipids was equilibrated in water for 1 μs, yielding the area per lipid of 60.7 ± 0.02 $Å^2$ at 308 K, in reasonable quantitative agreement with the experimental value of 60.8 ± 1.2 $Å^2$ at 303 K.[54]

Twelve peptides (12 PGLa or a mixture of 6 PGLa and 6 magainin 2) were placed above the equilibrated bilayer surface with a distance of ~2.4 nm between the peptide and bilayer centers, leading to the peptide/lipid molar ratio of 0.023, close to the recent NMR experimental condition.[31] To check the effect of the initial configuration, 12 peptides were aligned in parallel or antiparallel with different initial distributions (widely spaced or clustered), shown in Figure 2 and Table 1. These 12 peptides were added to both leaflets of the bilayer to obtain more sampling. The final simulation system consists of 24 peptides (12 peptides/leaflet), 512 DLPC lipids (256 lipids/leaflet), ~10300 CG water beads (representing ~41200 real waters), 96-120 counterions (Cl^-) in a periodic box of size 12.5 × 12.5 × 13 nm^3. A temperature of 308 K and a pressure of 1 bar were maintained by applying the velocity-rescale thermostat and Berendsen barostat in the $NP_{xy}P_zT$ ensemble (semi-isotropic pressure coupling).[55, 56] A real space cutoff of 12 Å was used for Lennard-Jones (LJ) and electrostatic forces. The LJ and coulomb potentials were smoothly shifted to zero between 9 and 12 Å, and between 0 and 12 Å, respectively. All simulations were performed for 7 μs with a time step of 20 fs on computational facilities supported by the National Institute of Supercomputing and Networking/Korea Institute of Science and Technology Information with supercomputing resources including technical support (KSC-2013-C2-46).

Results and Discussion

PGLa and magainin 2 were simulated in lipid bilayers for 7 μs. Simulated systems are

listed in Table 1, where "PGLa" and "PGLa-MAG" indicate the bilayer systems with only PGLa and those with the mixture of PGLa and magainin 2, respectively. The last two initials represent the initial orientation and distribution of a pair of peptides (dimer), where "a" and "p" respectively designate antiparallel and parallel orientations, and "s" and "c" respectively indicate "separated" and "clustered" distributions (Figure 2). Note that experiments have shown that PGLa form antiparallel homodimers by themselves,[57] while PGLa and magainin 2 form parallel heterodimers.[27] These orientations were applied as the initial orientations of peptides except that the PGLa-MAG-as system includes antiparallel dimers to check the effect of the initial orientation. To understand the dependence of dimer formation on the electrostatic interaction between magainin 2 and PGLa, magainin 2 was mutated by replacing anionic residues with neutral ones, named "-mMAG-".

Synergistic effect of magainin 2 on the insertion of PGLa into the bilayer

Figure 2 shows the initial and final snapshots of simulations. Starting with the position of peptides above the bilayer surface, peptides bind to the bilayer surface and insert into lipid bilayers. The deeper insertion of PGLa is observed for the system with PGLa and magainin 2 than for the system with only PGLa, implying the synergistic effect of PGLa and magainin 2. For the systems with mixtures of PGLa and magainin 2, magainin 2 interact mostly with lipid head groups and thus stay on the bilayer surface, while PGLa insert into the bilayer, presumably because PGLa has the larger hydrophobic surface than does magainin 2 (Figure 1). In Figure 3, as peptides insert into the bilayer, bilayer sizes increase and reach steady-state values at around 3 μs, indicating that simulations are equilibrated within the simulated time scale.

The insertion of peptides into the bilayer was further quantified by calculating the

distance between the bilayer center and the center of mass (COM) of each peptide in the bilayer normal direction (z-direction). In Figure 4, all the distances reach steady-state values within 3 μs, again indicating that simulations are well equilibrated, although distances fluctuate greatly. For the systems without magainin 2, most PGLa peptides are closely located in the lipid headgroup region, while for those with magainin 2 many PGLa peptides are much closer to the bilayer center, again indicating the synergistic effect of magainin 2 on the insertion of PGLa into the bilayer. Also, distances between magainin 2 and bilayer centers are very close to the distances between DLPC phosphate and bilayer centers, indicating that magainin 2 molecules interact with the bilayer surface and do no insert, consistent with Figure 2. These configurations of PGLa and magainin 2 in the bilayer are also confirmed by calculating mass densities. In Figure 5, PGLa-as and PGLa-ac (systems without magainin 2) show that most PGLa peptides are positioned around the bilayer surface, while other systems with a mixture of PGLa and magainin 2 show that PGLa peptides are in the hydrophobic region of lipid bilayers, consistent with Figures 2 and 4. Magainin 2 peptides are observed mostly in the DLPC-phosphate region, indicating that their strong electrostatic interactions with DLPC phosphates make magainin 2 stay on the bilayer surface. Figure 5 also shows less insertion of PGLa in PGLa-MAG-as and PGLa-mMAG-ps than in PGLa-MAG-ps and PGLa-MAG-pc, indicating the heterodimer formation and orientation of PGLa and magainin 2 influence the insertion of PGLa, which will be discussed in detail later. Here, our simulations show that the presence of magainin 2 promotes the deeper insertion of PGLa into the bilayer, indicating the synergistic effect, as also observed in experiments.[26, 29, 31, 32] In particular, extents of the insertion of PGLa and magainin 2 differ, which agrees well with recent NMR experiments that showed that PGLa insert into the bilayer, while magainin 2 stay on the bilayer surface.[31, 32]

Note that although the position and insertion extent of PGLa and magainin 2 in their mixtures agree with experiments,[32] our simulations with only PGLa peptides show that PGLa mostly stay on the surface of DLPC bilayers, which is different from experiments that showed the insertion of PGLa into the hydrophobic region of the DLPC bilayer.[32] This discrepancy may occur, since four methylene units are lumped into each CG tail-bead, and hence lipids with a difference of methylene units can be only semiquantitatively distinguished. To test this, we also simulated PGLa in the thinner bilayer, which has two CG beads per tail (recall that DLPC has three CG beads per tail). In Figure 6, density profiles and configurations clearly show the much deeper insertion of PGLa into the thinner bilayer, leading to the cross-membrane configuration, as observed in experiments.[32] These indicate that although the effect of the tail length cannot be accurately captured, simulations can reasonably reproduce the experimentally observed conformation of the inserted PGLa, which also supports the above-mentioned results of the insertion extent of PGLa and magainin 2 in their mixtures.

Dependence of insertion on the orientation of heterodimers

Experimentally, Tremouilhac et al. characterized the orientation of PGLa by measuring tilt angles of peptides in lipid bilayers,[29] which was defined as the angle between the z-axial vector (the bilayer normal) and the α-helical vector in the direction from N-terminal to C-terminal. Their NMR experiments showed that C-terminal groups of PGLa insert into the bilayer, leading to tilt angles of ~126° and ~158°, respectively, for the systems without and with magainin 2, indicating the more tilted orientation of PGLa in the presence of magainin 2. To quantify the peptide orientation and compare with experiments, tilt angles of simulated peptides were calculated. Here, the tilt angle is defined as the angle between the z-axis and the α-helical

axis of the peptide, where the α-helical axis in the upper leaflet is the vector connecting from the COM of backbone atoms of the 1^{st} ~ 4^{th} residues to the COM of backbone atoms of the last four residues, similar to the vector direction from N- to C-terminals in experiment.[29] For peptides in the lower leaflet of the bilayer, the α-helical vector was determined in the opposite direction (C- to N- terminals) to match tilt angles in the upper leaflet (Figure 7, top).

Figure 7 shows tilt angles of the 12 individual peptides for each system as a function of time. Magainin 2 peptides show lower tilt angles than do PGLa peptides, indicating the less tilted conformation of magainin 2, apparently because magainin 2 peptides interact with lipid headgroups and thus stay horizontally on the bilayer surface, as observed in Figures 4 and 5. All 12 PGLa peptides for each system (24 peptides for PGLa-as and PGLa-ac) were categorized according to their individual tilt angles in three different ranges of <105°, 106°~120°, and >121°, which are tabulated in Table 2. PGLa-MAG-ps and PGLa-MAG-pc show that more than half of the peptides are in the tilt-angle range of >121°, while other systems show that most peptides have the lower tilt angles, indicating that the parallel orientation of dimers and the charge interaction between PGLa and magainin 2 are important to increase the tilting of peptides.

These results indicate that the presence of magainin 2 significantly increase the tilting of PGLa, in qualitative agreement with Tremouilhac et al.'s NMR experiments,[29] although simulation and experimental values do not exactly match. Since the larger tilt angle of PGLa indicates deeper insertion into the bilayer, these results, combined with the observations in Figures 4 and 5, indicate that magainin 2 interact strongly with lipid headgroups and thus stay horizontally on the bilayer surface, while PGLa insert into the bilayer, leading to the tilted orientation. In particular, PGLa is less tilted in the system with the initially antiparallel heterodimer orientation (PGLa-MAG-as) or with mutated magainin 2 (PGLa-mMAG-ps),

indicating that the parallel orientation and the stronger electrostatic interaction between magainin 2 and PGLa induce deeper insertion of PGLa, which agrees with the Matsuzaki group's experiments that showed the greater extent of antimicrobial activity for parallel heterodimers.[27,28]

Interactions of PGLa and magainin 2 with lipid bilayers

As discussed above, our simulations show that the positions of PGLa and magainin 2 differ in the bilayer, indicating that they may not form heterodimers. However, simulations also show that the parallel heterodimer and the strong charge interaction between PGLa and magainin 2 significantly increase the extent of PGLa insertion. Thus, these two simulation findings seem to conflict. Note that experiments have also shown the formation of parallel heterodimers in the presence of magainin 2,[27] as well as different positions of PGLa and magainin 2.[31, 32] To understand these conflicting observations and the mechanism for the synergistic effect, the interactions of PGLa and magainin 2 with lipid bilayers were analyzed.

Figure 8 shows the number of "clusters" of peptides as a function of time, where a cluster is either a complex of any size or a free peptide. Here, if the distance between beads of different peptides is less than 0.5 nm, then those are considered to be a cluster. Other criteria with the distance from 0.6 to 0.8 nm produce similar qualitative trends. Figure 8 also shows the number of peptides in the largest cluster as a function of time. These both reach steady-state values at ~3 μs, indicating the formation of the equilibrated complexes in the bilayer. Peptides are much more complexed in the systems with magainin 2 than in those without magainin 2 (PGLa-as and PGLa-ac). In particular, more than 7-8 peptides are clustered for each leaflet, leading to the largest complex with 14-16 peptides, similar to the pore formation, as visualized in Figure 8. Figure 9 shows radial distribution functions (RDFs) between anionic phosphates of

DLPC and cationic residues of PGLa. The systems without magainin 2 (PGLa-as and PGLa-ac) or with mutated magainin 2 (PGLa-mMAG-ps) show the higher peaks than do others, indicating the stronger charge interactions between PGLa and lipid headgroups, which can inhibit the PGLa insertion. These imply that magainin 2 peptides induce the clustering of peptides, which may help the deeper insertion of PGLa.

To understand the interaction of heterodimers in the peptide complex visualized in Figure 8, we calculated RDFs of five cationic residues of the clustered PGLa with respect to two anionic residues (Glutamic acid (19Glu) and C-terminal (23Ser)) of magainin 2 in the complex. Recall from Figure 1 that magainin 2 consists of two anionic and five cationic residues, while PGLa consists of only five cationic residues. Experiments suggested that parallel heterodimers are induced by the electrostatic interactions between anionic residues of magainin 2 and cationic residues of PGLa.[29] Figure 10 shows that the 19Glu residues of magainin 2 mostly interact with 12^{th}, 15^{th}, and 19^{th} lysines (Lys) of PGLa, and that 23Ser residues of magainin 2 interact with 15^{th} and 19^{th} Lys of PGLa, indicating the formation of parallel heterodimers in the peptide complex, as shown in experiments.[27] These results are observed only in the simulations PGLa-MAG-ps and PGLa-MAG-pc, which show the deepest insertion and the most tilted orientation of PGLa. Note that when peptides were initially aligned in antiparallel (PGLa-MAG-as) or mutated with neutral residues (PGLa-mMAG-ps), much fewer parallel dimers form, leading to less insertion and tilted orientation of PGLa. These indicate that magainin 2 peptides form parallel heterodimers with PGLa and induce the aggregation of heterodimers, where magainin 2 stay on the bilayer surface, but PGLa insert into the bilayer.

These simulation results, combined with observations in Figures 4-7, support the experimental observations and suggestions. Parallel heterodimers of PGLa and magainin 2

promote more tilting and insertion of PGLa into the bilayer than do antiparallel heterodimers or only PGLa peptides, indicating that the parallel orientation of heterodimers is important for the insertion of PGLa, in agreement with experiments that showed the formation of magainin 2-PGLa heterodimers and their synergistic effects on insertion.[27, 28] Also, magainin 2 peptides tend to stay on the bilayer surface, while PGLa peptides insert into the bilayer, which also qualitatively agrees with solid-state MNR experiments.[31, 32] In particular, magainin 2 induces the aggregation of parallel heterodimers, which may be important for stable pore formation, as suggested from experiments.[26,28,29] These findings explain the conflicting experimental observations of the heterodimer formation as well as different positions of PGLa and magainin 2 in the bilayer. PGLa and magainin 2 form parallel heterodimers and aggregate in the bilayer, leading to the formation of pores, where magainin 2 peptides tend to interact with the bilayer surface, while PGLa peptides insert into the hydrophobic region of the bilayer, which allows PGLa to be more tilted. To more carefully check the stability of parallel heterodimers in the peptide complex, all-atom simulation studies of the interaction between magainin 2 and PGLa ought to be performed, which we hope to report on elsewhere.

Conclusions

PGLa and magainin 2 were simulated with lipid bilayers using the coarse-grained model to complement the experimentally observed positions and conformations of peptides, as well as to understand their synergistic effects on the peptide aggregation and insertion into the bilayer. The bilayer systems include either only PGLa peptides or the mixture of PGLa and magainin 2 (molar ratio of 1:1), which were initially widely spaced or clustered above the bilayer surface. PGLa more deeply insert into the bilayer for the systems with magainin 2 than for those without

magainin 2, indicating the synergistic effect of the PGLa-magainin heterodimers on the PGLa insertion. Magainin 2 peptides have the strong charge interaction with lipid headgroups and thus mostly stay on the bilayer surface, while PGLa peptides are tilted and inserted into the bilayer, in agreement with recent NMR experiments that showed different positions and insertion extents of magainin 2 and PGLa in membranes. Interestingly, when heterodimers are initially aligned in antiparallel or with the neutrally mutated magainin 2, much fewer heterodimers form, showing the less tilted conformation. This indicates that PGLa and magainin 2 tend to form parallel heterodimers, which can induce the deeper insertion and more tilted conformation of PGLa, as observed in experiments. Also, peptides are clustered and then inserted into the bilayer with the mixture of PGLa and magainin 2, but they are not even clustered in the system with only PGLa.

Although simulations capture the experimentally observed conformation and insertion extent of PGLa and magainin 2 in lipid bilayers, the pore formation was not explicitly observed over our simulation time scale. Despite this, simulations show that PGLa and magainin 2 form parallel heterodimers, and that magainin 2 and PGLa are positioned respectively on the bilayer surface and in the hydrophobic region of the bilayer, leading to the tilted conformation of PGLa. In particular, the extents of the PGLa insertion and tilting increase only in the presence of parallel heterodimers, showing the dependence of the PGLa insertion on the formation of parallel heterodimers, as observed in experiments. These indicate that leakage or even pore formation could well eventually occur in the systems with the mixture of PGLa and magainin 2, since experiments have shown that magainin 2-PGLa heterodimers and their tilting conformations induce more stable pore formation than do PGLa without magainin 2.[26,28,29] Also, note that the heterodimer formation and different positions of PGLa and magainin 2 seem to conflict. Our simulations show that heterodimers aggregate, but PGLa peptides (without magainin 2) do not

aggregate, indicating that magainin 2 induce the peptide aggregation, which may play an important role in pore formation. Thus, heterodimers form, aggregate, and induce pore formation, where magainin 2 are positioned on the bilayer surface, while PGLa are more tiled and inserted into the bilayer, which helps explain the conflicting experimental observations.

Acknowledgments

This research was supported by Basic Science Research Program through the National Research Foundation of Korea (NRF) funded by the Ministry of Education (NRF-2014R1A1A2054016).

References

1. M. Zasloff, *Nature*, 2002, 415, 389-395.
2. R. M. Epand and H. J. Vogel, *Biochimica et biophysica acta*, 1999, 1462, 11-28.
3. M. R. Yeaman and N. Y. Yount, *Pharmacol. Rev.*, 2003, 55, 27-55.
4. R. E. W. Hancock and H. G. Sahl, *Nature Biotechnology*, 2006, 24, 1551-1557.
5. R. E. W. Hancock, *The Lancet infectious diseases*, 2001, 1, 156-164.
6. Y. Imura, M. Nishida and K. Matsuzaki, *Biochimica et biophysica acta*, 2007, 1768, 2578-2585.
7. Y. Imura, M. Nishida, Y. Ogawa, Y. Takakura and K. Matsuzaki, *Biochimica et biophysica acta*, 2007, 1768, 1160-1169.
8. T. Doherty, A. J. Waring and M. Hong, *Biochimica et Biophysica Acta - Biomembranes*, 2006, 1758, 1285-1291.
9. K. Hilpert, M. R. Elliott, R. Volkmer-Engert, P. Henklein, O. Donini, Q. Zhou, D. F. H. Winkler and R. E. W. Hancock, *Chemistry and Biology*, 2006, 13, 1101-1107.
10. M. T. Lee, W. C. Hung, F. Y. Chen and H. W. Huang, *Proceedings of the National Academy of Sciences of the United States of America*, 2008, 105, 5087-5092.
11. R. Mani, S. D. Cady, M. Tang, A. J. Waring, R. I. Lehrer and M. Hong, *Proceedings of the National Academy of Sciences of the United States of America*, 2006, 103, 16242-16247.
12. S. Kobayashi, K. Takeshima, C. B. Park, S. C. Kim and K. Matsuzaki, *Biochemistry*, 2000, 39, 8648-8654.
13. N. Sitaram and R. Nagaraj, *Biochimica et Biophysica Acta - Biomembranes*, 1999, 1462, 29-54.

14. L. M. Gottler and A. Ramamoorthy, *Biochimica et Biophysica Acta - Biomembranes*, 2009, 1788, 1680-1686.

15. B. Bechinger, *Biochimica et Biophysica Acta - Biomembranes*, 1999, 1462, 157-183.

16. K. Matsuzaki, *Biochimica et Biophysica Acta - Biomembranes*, 2009, 1788, 1687-1692.

17. V. Teixeira, M. J. Feio and M. Bastos, *Progress in lipid research*, 2012, 51, 149-177.

18. I. Nagaoka, S. Hirota, S. Yomogida, A. Ohwada and M. Hirata, *Inflammation Research*, 2000, 49, 73-79.

19. S. Kobayashi, Y. Hirakura and K. Matsuzaki, *Biochemistry*, 2001, 40, 14330-14335.

20. H. Yan and R. E. W. Hancock, *Antimicrobial agents and chemotherapy*, 2001, 45, 1558-1560.

21. Y. Rosenfeld, D. Barra, M. Simmaco, Y. Shai and M. L. Mangoni, *Journal of Biological Chemistry*, 2006, 281, 28565-28574.

22. A. Mor, K. Hani and P. Nicolas, *Journal of Biological Chemistry*, 1994, 269, 31635-31641.

23. R. W. Williams, R. Starman, K. M. Taylor, K. Gable, T. Beeler, M. Zasloff and D. Covell, *Biochemistry*, 1990, 29, 4490-4496.

24. A. Vaz Gomes, A. de Waal, J. A. Berden and H. V. Westerhoff, *Biochemistry*, 1993, 32, 5365-5372.

25. H. V. Westerhoff, M. Zasloff, J. L. Rosner, R. W. Hendler, A. De Waal, A. Vaz Gomes, P. M. Jongsma, A. Riethorst and D. Juretic, *European journal of biochemistry / FEBS*, 1995, 228, 257-264.

26. K. Matsuzaki, Y. Mitani, K. Y. Akada, O. Murase, S. Yoneyama, M. Zasloff and K. Miyajima, *Biochemistry*, 1998, 37, 15144-15153.

27. T. Hara, Y. Mitani, K. Tanaka, N. Uematsu, A. Takakura, T. Tachi, H. Kodama, M. Kondo, H. Mori, A. Otaka, F. Nobutaka and K. Matsuzaki, *Biochemistry*, 2001, 40, 12395-12399.

28. M. Nishida, Y. Imura, M. Yamamoto, S. Kobayashi, Y. Yano and K. Matsuzaki, *Biochemistry*, 2007, 46, 14284-14290.

29. P. Tremouilhac, E. Strandberg, P. Wadhwani and A. S. Ulrich, *Journal of Biological Chemistry*, 2006, 281, 32089-32094.

30. E. Strandberg, P. Tremouilhac, P. Wadhwani and A. S. Ulrich, *Biochimica et biophysica acta*, 2009, 1788, 1667-1679.

31. E. Strandberg, J. Zerweck, P. Wadhwani and A. S. Ulrich, *Biophysical journal*, 2013, 104, L9-L11.

32. E. S. Salnikov and B. Bechinger, *Biophysical journal*, 2011, 100, 1473-1480.

33. S. K. Kandasamy and R. G. Larson, *Chemistry and physics of lipids*, 2004, 132, 113-132.

34. M. Mihajlovic and T. Lazaridis, *Biochimica et biophysica acta*, 2012, 1818, 1274-1283.

35. H. Leontiadou, A. E. Mark and S. J. Marrink, *Journal of the American Chemical Society*, 2006, 128, 12156-12161.

36. K. P. Santo and M. L. Berkowitz, *Journal of Physical Chemistry B*, 2012, 116, 3021-3030.

37. A. J. Rzepiela, D. Sengupta, N. Goga and S. J. Marrink, *Faraday discussions*, 2009, 144, 431-443.

38. H. J. Woo and A. Wallqvist, *Journal of Physical Chemistry B*, 2011, 115, 8122-8129.

39. L. Monticelli, S. K. Kandasamy, X. Periole, R. G. Larson, D. P. Tieleman and S. J. Marrink, *Journal of Chemical Theory and Computation*, 2008, 4, 819-834.

40. H. Khandelia, J. H. Ipsen and O. G. Mouritsen, *Biochimica et Biophysica Acta - Biomembranes*, 2008, 1778, 1528-1536.

41. E. Matyus, C. Kandt and D. P. Tieleman, *Current medicinal chemistry*, 2007, 14, 2789-2798.

42. S. K. Kandasamy and R. G. Larson, *Biochimica et Biophysica Acta - Biomembranes*, 2006, 1758, 1274-1284.

43. E. Han and H. Lee, *Langmuir : the ACS journal of surfaces and colloids*, 2013, 29, 14214-14221.

44. J. P. Ulmschneider, J. C. Smith, M. B. Ulmschneider, A. S. Ulrich and E. Strandberg, *Biophysical journal*, 2012, 103, 472-482.

45. B. Hess, C. Kutzner, D. Van Der Spoel and E. Lindahl, *Journal of Chemical Theory and Computation*, 2008, 4, 435-447.

46. S. Pronk, S. Pall, R. Schulz, P. Larsson, P. Bjelkmar, R. Apostolov, M. R. Shirts, J. C. Smith, P. M. Kasson, D. van der Spoel, B. Hess and E. Lindahl, *Bioinformatics*, 2013, 29, 845-854.

47. E. Lindahl, B. Hess and D. van der Spoel, *Journal of Molecular Modeling*, 2001, 7, 306-317.

48. D. Van Der Spoel, E. Lindahl, B. Hess, G. Groenhof, A. E. Mark and H. J. C. Berendsen, *Journal of Computational Chemistry*, 2005, 26, 1701-1718.

49. S. J. Marrink, A. H. De Vries and A. E. Mark, *Journal of Physical Chemistry B*, 2004, 108, 750-760.

50. S. J. Marrink, H. J. Risselada, S. Yefimov, D. P. Tieleman and A. H. De Vries, *Journal of Physical Chemistry B*, 2007, 111, 7812-7824.

51. D. H. De Jong, G. Singh, W. F. D. Bennett, C. Arnarez, T. A. Wassenaar, L. V. Schäfer, X. Periole, D. P. Tieleman and S. J. Marrink, *Journal of Chemical Theory and Computation*,

2013, 9, 687-697.

52. T. Wieprecht, O. Apostolov, M. Beyermann and J. Seelig, *Biochemistry*, 2000, 39, 442-452.

53. B. Bechinger, M. Zasloff and S. J. Opella, *Protein Science*, 1993, 2, 2077-2084.

54. N. Kučerka, M. P. Nieh and J. Katsaras, *Biochimica et Biophysica Acta - Biomembranes*, 2011, 1808, 2761-2771.

55. G. Bussi, D. Donadio and M. Parrinello, *Journal of Chemical Physics*, 2007, 126.

56. H. J. C. Berendsen, J. P. M. Postma, W. F. Van Gunsteren, A. Dinola and J. R. Haak, *The Journal of chemical physics*, 1984, 81, 3684-3690.

57. R. W. Glaser, C. Sachse, U. H. N. Dürr, P. Wadhwani, S. Afonin, E. Strandberg and A. S. Ulrich, *Biophysical journal*, 2005, 88, 3392-3397.

58. W. Humphrey, A. Dalke and K. Schulten, *Journal of Molecular Graphics*, 1996, 14, 33-38.

Table 1. List of simulations.

	No. of molecules			Initial orientation of peptides	Initial distribution of peptides	Simulation time (μs)
	PGLa	Magainin 2	DLPC			
PGLa-as	24	-	512	antiparallel	separated	7
PGLa-ac	24	-	512	antiparallel	clustered	7
PGLa-MAG-ps	12	12	512	parallel	separated	7
PGLa-MAG-pc	12	12	512	parallel	clustered	7
PGLa-MAG-as	12	12	512	antiparallel	separated	7
PGLa-mMAG-ps	12	12	512	parallel	separated	7

Table 2. Number of PGLa peptides according to their individual tilt angles.

	No. of PGLa in terms of the tilt angle		
	< 105°	106° ~ 120°	121°<
PGLa-as	9	15	-
PGLa-ac	3	21	-
PGLa-MAG-ps	-	5	7
PGLa-MAG-pc	2	3	7
PGLa-MAG-as	3	8	1
PGLa-mMAG-ps	4	8	-

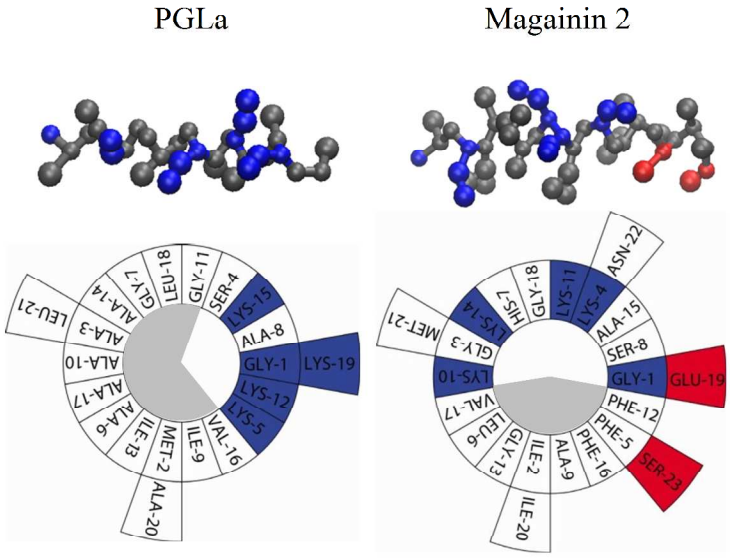

Figure 1. Structures and helical wheel diagrams for PGLa (left) and magainin 2 (right). Gray, red and blue colors represent hydrophobic, anionic and cationic residues, respectively. For the wheel diagram, amino acid sequences are plotted clockwise. The structure images were created using Visual Molecular Dynamics.[58]

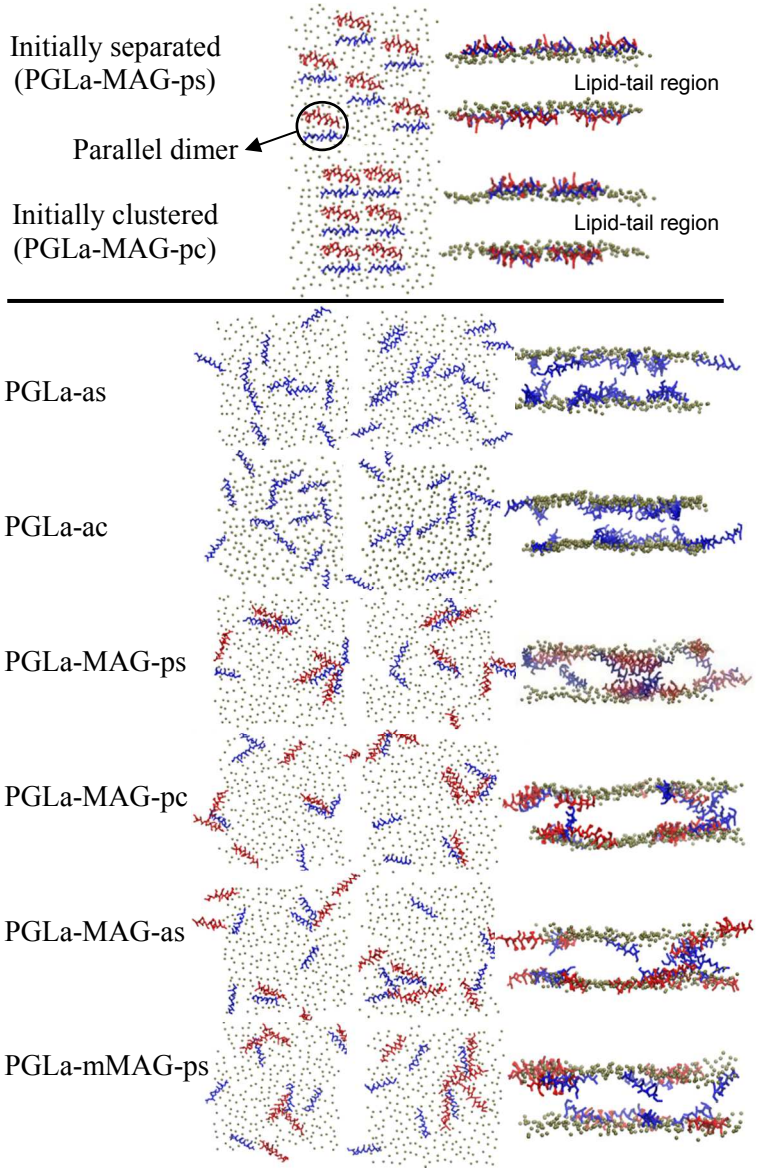

Figure 2. Snapshots at the beginning (0 μs, rows 1 and 2) and end (7 μs, rows 3-8) of simulations. For the final configurations, top views for each leaflet (left and middle images), and side views (right images) are shown. Initial configurations are shown only for PGLa-MAG-ps and PGLa-MAG-pc, but this peptide distribution (either widely spaced or clustered) is also used for other systems. Blue, red, and brown colors respectively represent PGLa, magainin 2, and DLPC phosphates, while DLPC tails, water, and ions are omitted for clarity. Note that side views show only one cross-section of the system and cannot capture all peptides.

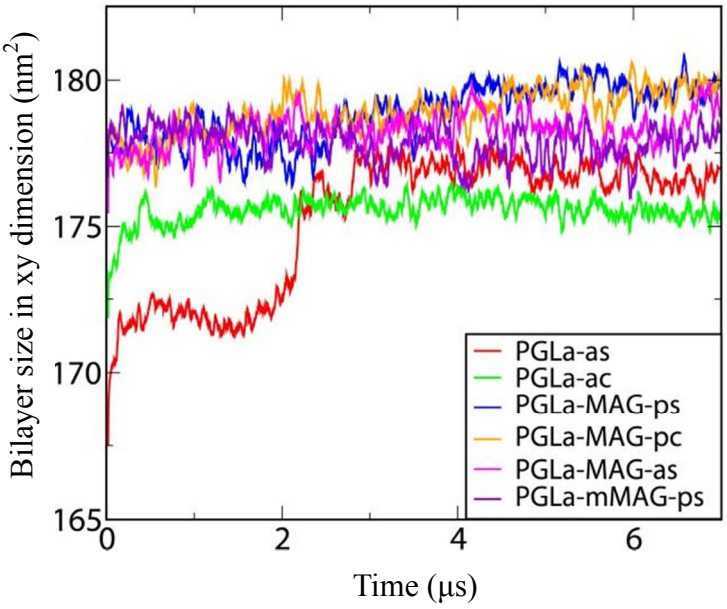

Figure 3. The bilayer size in xy dimension as a function of time.

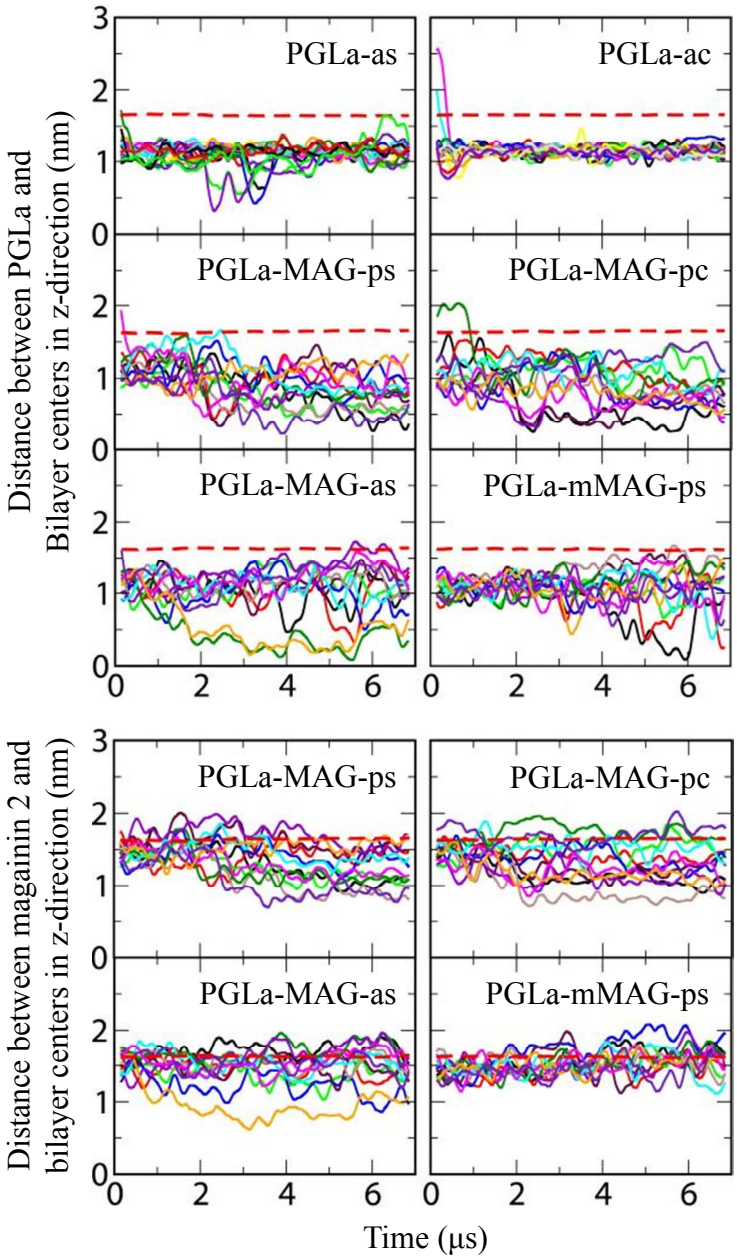

Figure 4. Distances between centers of mass (COM) of each peptide and the bilayer in the bilayer normal direction (z-direction) as a function of time (PGLa and magainin 2, respectively, in top and bottom panels). Dotted red lines represent the distance between COMs of DLPC phosphates and the bilayer, and solid lines with different colors designate the distance for the COM of each peptide.

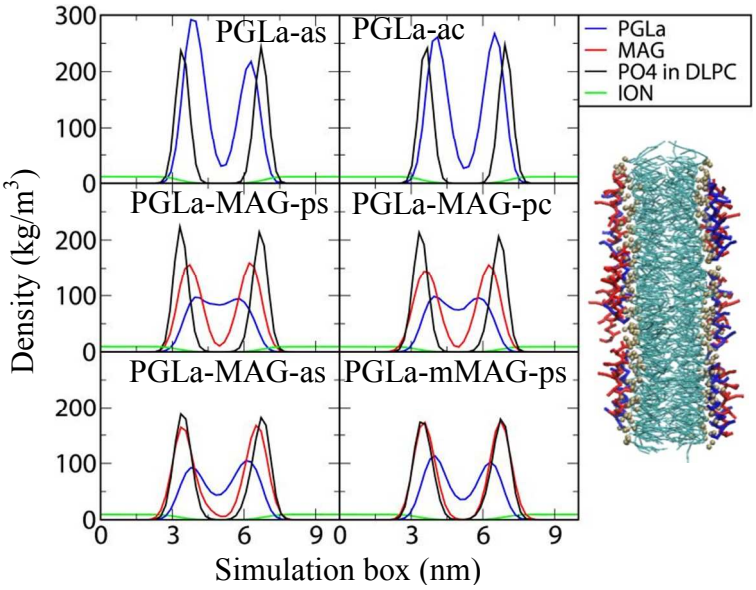

Figure 5. Mass density profiles of peptides, DLPC lipids, and Cl^- ions.

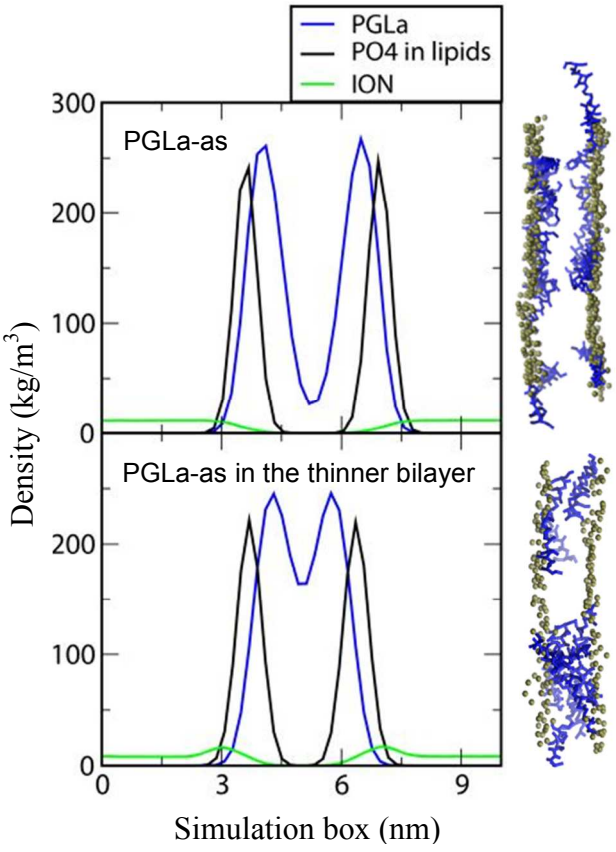

Figure 6. Mass density profiles of peptides, DLPC lipids, and Cl^- ions for the systems composed of 24 PGLa peptides in the DLPC bilayer (PGLa-as; top) and those in the thinner bilayer (bottom).

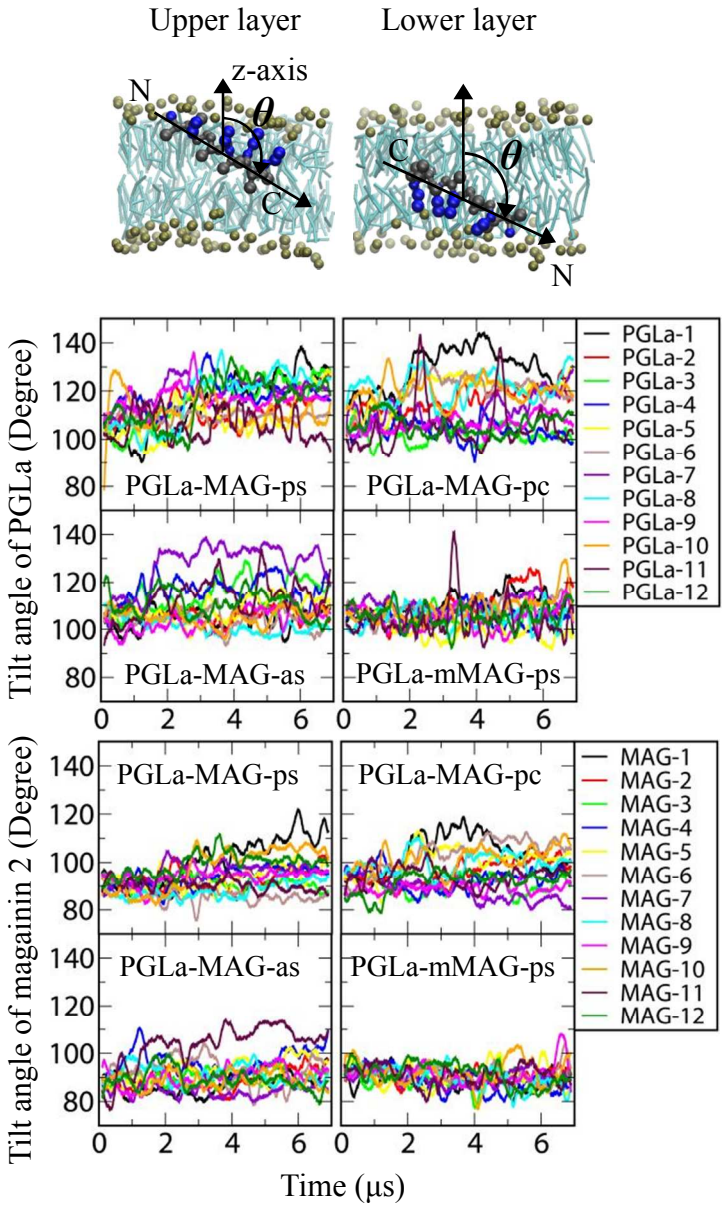

Figure 7. Tilt angles of individual 12 peptides for PGLa (top) and magainin 2 (bottom) as a function of time. Tilt angles were computed by measuring the angle between α-helix of the peptide and the z-axis.

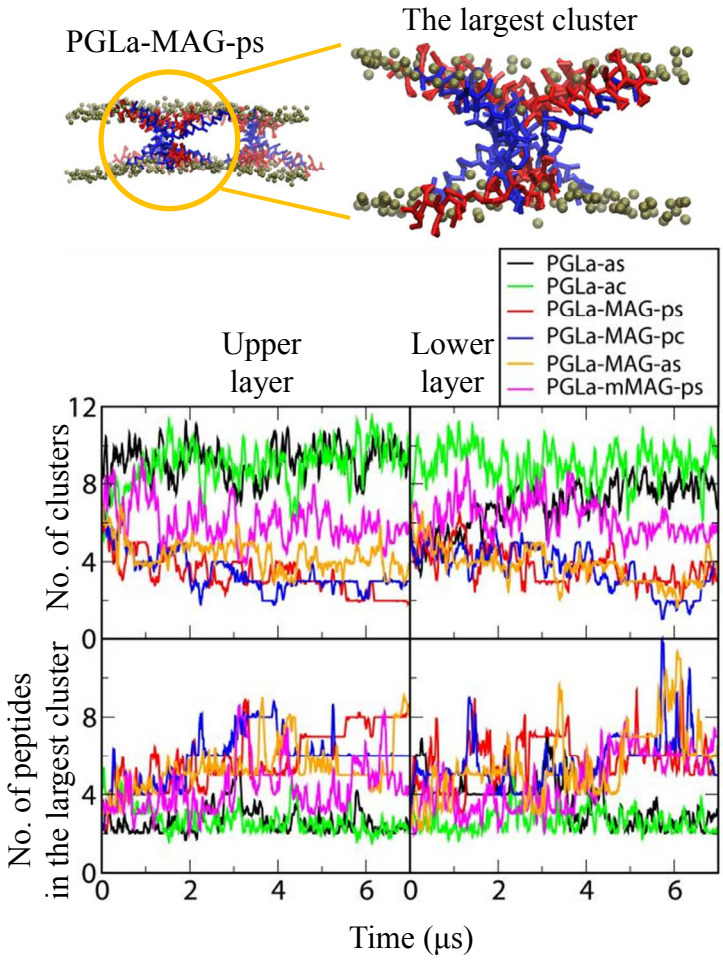

Figure 8. Number of "clusters", where a "cluster" is an aggregate of any size, including single peptides (top), and number of aggregated peptides in the largest cluster (bottom) as a function of time.

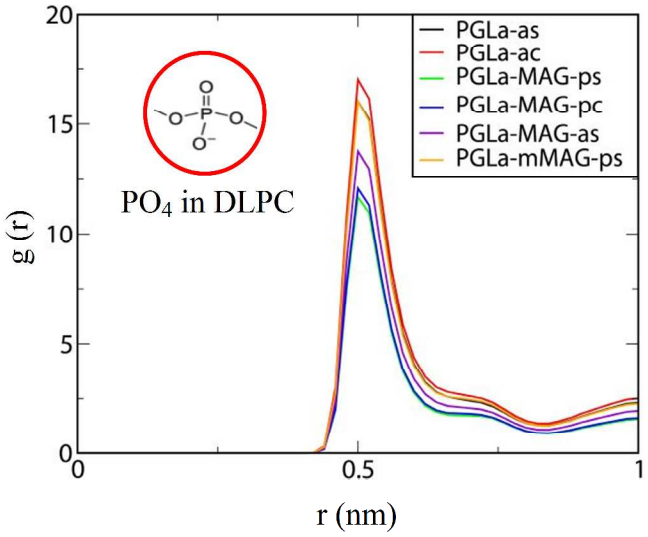

Figure 9. Radial distribution functions between anionic DLPC phosphates and cationic residues of PGLa.

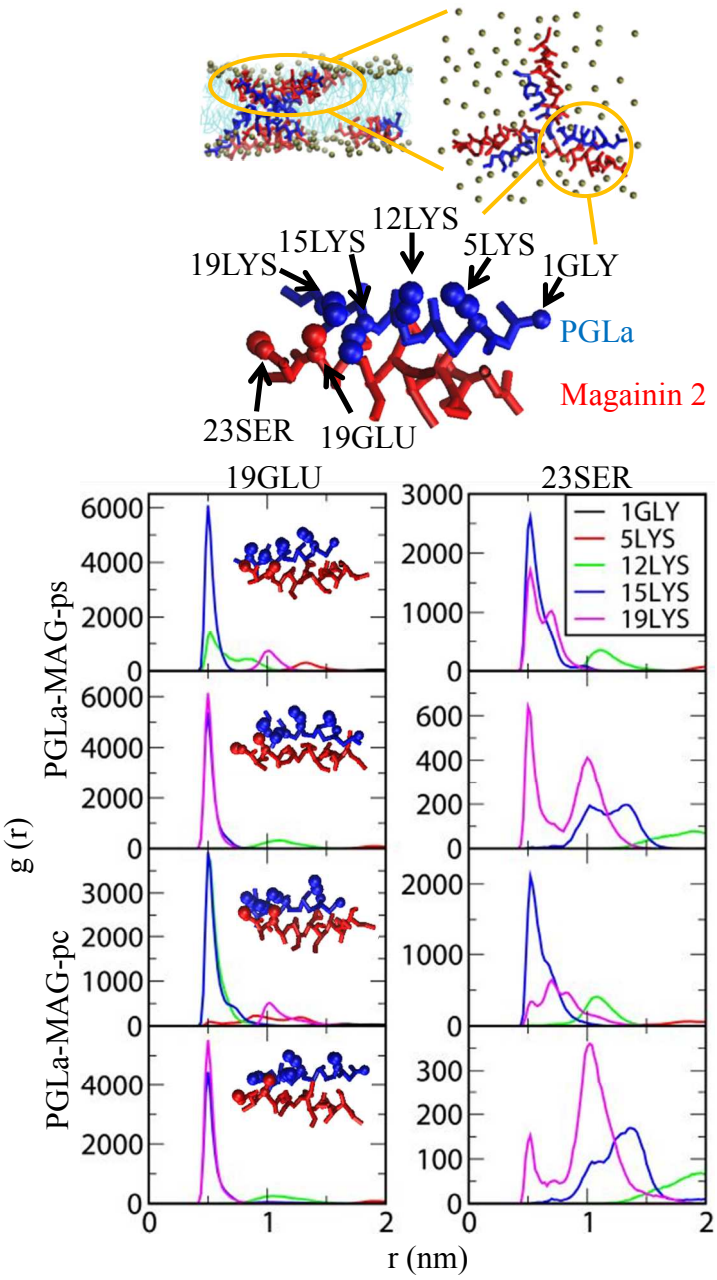

Figure 10. Radial distribution functions of cationic residues of PGLa with respect to anionic residues of magainin 2. In the schematic illustration of parallel heterodimers, magainin 2 and PGLa are colored in red and blue, respectively.

For Table of Contents only

Title: Synergistic Effects of Magainin 2 and PGLa on Their Heterodimer Formation, Aggregation, and Insertion into the Bilayer

Authors: Eol Han, Hwankyu Lee